ANALYTICAL ELECTRON MICROSCOPY EXAMINATION OF URANIUM CONTAMINATION AT THE DOE FERNALD OPERATION SITE

E. C. Buck, N. L. Dietz, J. K. Bates and J. C. Cunnane
Chemical Technology Division
Argonne National Laboratory, Argonne, IL 60439

ABSTRACT

Analytical Electron Microscopy (AEM) has been used to identify uranium-bearing phases present in contaminated soils from the DOE Fernald operation site. A combination of optical microscopy, scanning electron microscopy with backscattered electron detection (SEM/BSE), and AEM was used in isolating and characterizing uranium-rich regions of the contaminated soils. Soil samples were prepared for transmission electron microscopy (TEM) by ultramicrotomy using an embedding resin previously employed for aquatic colloids and biological samples. This preparation method allowed direct comparison between SEM and TEM images. At the macroscopic level much of the uranium appears to be associated with clays in the soils; however, electron beam analysis revealed that the uranium is present as discrete phases, including iron oxides, silicates (soddyite), phosphates (autunites), and fluorite. Only low levels of uranium were actually within the clay minerals. The distribution of uranium phases was inhomogeneous at the submicron level.

INTRODUCTION

Technologies are under development for remediating the uranium-contaminated soils resulting from defense-related operations at the Fernald Environmental Management Project Site, OH. These remediation technologies begin with characterization of the nature and distribution of the uranium contamination, followed by the application of chemical and physical separation technologies (1). Analytical Electron Microscopy (AEM) is one tool that can be used to determine the nature of uranium interactions with the local environment at the submicron level. Such interactions, termed weathering, will affect the transportability of uranium in the groundwater system. Uranium weathering results in the transformation of the primary uranium-bearing phases into secondary minerals or incorporation of uranium into other phases (2). Such phases can be identified with the combination of techniques available with AEM, including imaging, electron diffraction, X-ray energy dispersive spectroscopy (EDS), and electron energy loss spectroscopy (EELS).

At Fernald, the contamination of the soil generally came from three sources; airborne uranium dust particles, aqueous uranium wastes, and solid uranium product spills (3). An extensive sampling program has identified the areas of major contamination, and current interest is on further analysis of selected samples from the site. In this investigation soil fractions taken from two different sampling positions (SP) have been analyzed. One fraction was analyzed from SP4 (Plant 1/Storage Pad Area) and was taken from a core sample from a depth of 8.5 cm. The contamination in this area resulted mainly from uranium product spills. The second sample SP10 (taken in the vicinity of the Fernald incinerator plant), had had its uranium content concentrated by a gravimetric method, and it was the concentrated sample which was analyzed by AEM.

The basic components of the contaminated soils had been earlier identified by SEM and x ray diffraction as various clays and quartz, and revealed the presence of uranium inclusions associated with the clay fraction of the soil, but a unique description of the phases was not provided (3). This paper describes the characterization of the uranium-bearing soil fractions from Fernald sites including both processed and untreated soil. The objective of the paper is to (a) describe the combination of optical microscopy, Scanning Electron Microscopy using Backscattering Electrons (SEM/BSE), and AEM as a coherent methodology to provide representative characterization data on the uranium-bearing phases within the contaminated soil, and (b) to identify discrete uranium phases found in Fernald soil fractions.

EXPERIMENTAL

The uranium-bearing phases in the contaminated soil samples were isolated using micromanipulation techniques assisted by polarizing light microscopy and SEM/BSE. Thin sections for Transmission Electron Microscopy (TEM) analysis were produced by ultramicrotomy. AEM was performed using a JEOL 2000FXII TEM operated at 200 kV.

Thin sectioning of isolated small particulates by ultramicrotomy is well described in the literature (4,5). Thin sections of soil constituents have been prepared using the microtome, but the technique has seen limited use in gross soil studies. Wada and Kakuto (6) have examined clays in soils by TEM, producing samples by embedding them in epoxy and then sectioning.

In studies where a representative sample of the bulk is required, it is necessary to show that one is observing the same regions in the SEM and the TEM. This has usually been a difficult task to accomplish, as it requires producing an intact sample section along a precise direction and over a specific area. Comparison of SEM and TEM images allows greater confidence in determining whether uranium-bearing phases are not just peculiarities, but true representations of the major uranium-bearing phases in the soil.

To provide a representative characterization of uranium phases distributed in soil, a relatively large number of unaltered soil particles must be examined. This was achieved by mounting particles for SEM and examining polished cross sections with a backscattered electron detector. Because the objective was to use an embedding resin that would allow thin sectioning of a uranium-containing particle directly from the SEM mount, it was imperative to use a resin with optimum infiltration and sectioning properties.

Ultramicrotomy of soil particles is the most appropriate means of viewing the undisturbed spatial relationship of soil components. Section quality can be substantially improved by selecting a resin that has good cohesion and matched hardness

with the sample, and several different embedding media were evaluated. The best improvement in infiltration was achieved with a water-soluble melamine resin, which is used to replace water in wetted soil particles. Frösch et al. (7) compared sections made of the polar melamine resin and a non-polar epoxide resin and found that the melamine resin produces much thinner and smoother sections. The soil particles were prepared for microtomy following a procedure similar to that used in the preparation of aquatic colloids (8).

The SEM results showed an improvement in the polished surface and in the infiltration of large particles with the melamine resin. Because the spatial relationship of uranium phases within the larger particles was well preserved, more uranium-containing areas could be isolated in a given field of view. The increased section quality made it possible to produce completely intact sections thinner than sections obtained with the epoxy and acrylic resins. Because of these improvements, the uranium phases identified in the TEM could be correlated with the corresponding areas in the SEM/BSE image.

In Fig. 1, structures from the same particle can be seen in both the SEM and TEM micrographs. The slight discrepancy in particle morphology between the SEM and TEM images is due to the sectioning process, which may occur over a depth of ~3 μm; however, the overall structure of the particles is preserved.

RESULTS AND DISCUSSION

While the general mineralogy of the soil samples has been described by Lee and Marsh (3), we sought to identify the specific phases in the current samples and thereby determine the distribution of uranium within the clay fraction of the soils. The TEM examination of the soils revealed two major components, quartz and clay. In Fig. 2, a quartz particle can be seen surrounded by clay particles. Clays mineral types in SP4 were identified as mica, chlorite, and smectite clay groups by selected area electron diffraction (SAED), EDS composition data, and clay morphology. However, specific clay minerals could not be identified with the method of analysis used.

Clay minerals are known to have an affinity for uranyl species and take up uranium either by adsorption onto the surface of the clay or within interlayer sites (9). The affinity for cation sorption depends on the clay mineralogy and the nature of the cation which compensates for the negative surface charge. At Fernald, bulk analyses of soil samples has suggested that uranium is associated with clay phases, based on gross studies of the large soil fraction. In the present study, a mica group clay was found to contain no detectable uranium, but a small amount of uranium (< 1 wt%) was found to be associated, on occasions, with a chlorite group clay. At times it appeared that a high concentration of uranium was present in the clay minerals, but this was later identified as a discrete uranium silicate phase (see Fig. 3). The SAED patterns from this phase were consistent with soddyite [$(UO_2)_2(SiO_4) \bullet 2H_2O$], a uranyl silicate commonly found as an alteration product both in laboratory-reacted and field-weathered uraninite (10, 11). The presence of this phase in the core soil sample SP4 suggests some weathering of the uranium.

For sample SP4, calcium and uranium were detected together in a number of SEM analyses, which indicated that this phase was an important uranium-bearing phase (see Fig. 4) The calcium phase, though crystalline, consisted of many small crystallites, resulting in a powdered SAED pattern, which matched with fluorite. Compositional analysis by EELS confirmed that oxygen was not a major component of this phase.

Amorphous uranium-bearing iron oxide phases were observed in many regions of sample SP4 (Fig. 5). This type of uranium phase had a different morphology compared to that of the calcium phase. It consisted of small (100 nm diameter) particles, which often appeared to be strung together into a much larger agglomerate. A higher concentration of uranium was found in the iron uranium oxide phase than in the calcium fluoride phase. The uranium concentration varied considerably, suggesting the adsorption of uranium on the iron oxide particles. Hsi and Langmuir have observed the pH-dependent adsorption of uranyl [U(VI)] on various iron oxides (12).

Uranium oxide particles were found in both the processed soil from SP10 and, less frequently, in the core samples from SP4. The SAED of uranium oxide phases found in SP4, located in the vicinity of the calcium fluoride phase described earlier, matched that of fluorite. A uranium phosphate phase was found in one group of particles in SP4. The phase was crystalline judging from the morphology; however, SAED analysis failed to detect any signs of crystallinity. The uranium phosphate particles were elongated and micrographs appeared to display lattice fringes. In SP10 the second major phase found was a uranium phosphate phase. In Fig. 6, long fibrous particles of the uranium phosphate phase can be

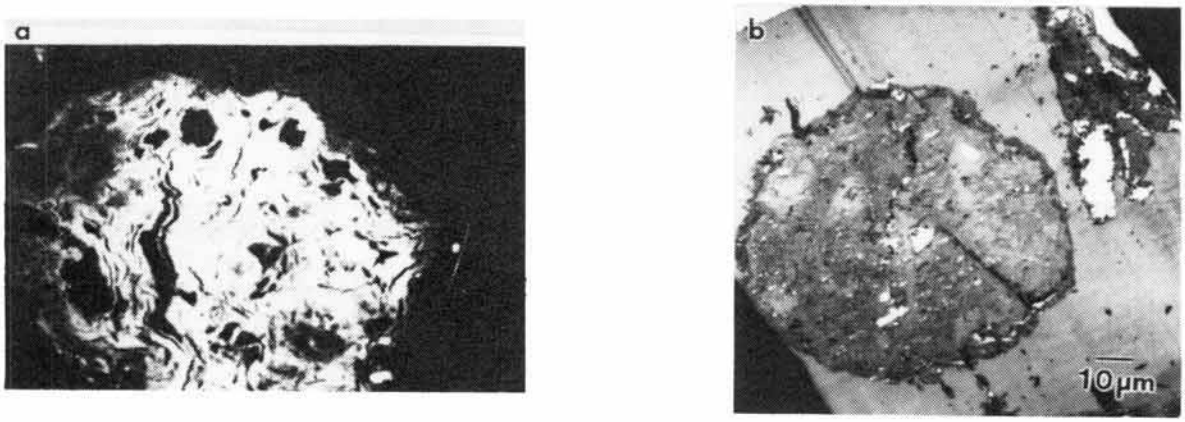

Fig. 1. (a) SEM/BSE micrograph showing round particles, which can also be seen in the (b) TEM image. The uranium-contaminated regions are identified by the white BSE contrast. The particles are similar in shape because the SEM mount has been sectioned nearly parallel to the plane of the paper.

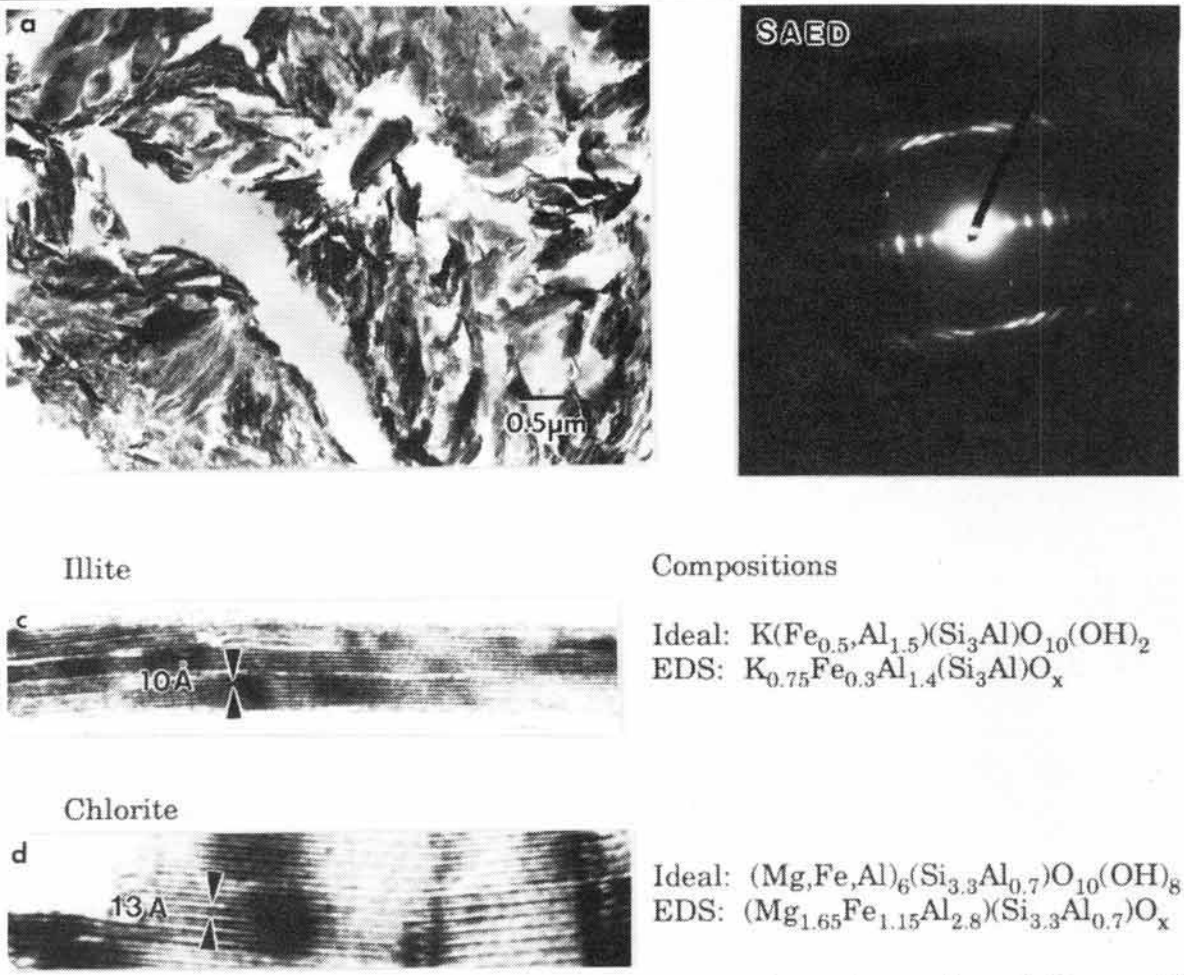

Fig. 2. (a) Low magnification micrograph of sectioned soil sample showing clays and quartz (arrow). Electron diffraction of sectioned clays often revealed textured patterns (b), in this case, a chlorite type clay. Lattice images of (c) illite and (d) chlorite (vermiculite) with c-axis spacings of ~10Å and ~13-14Å, respectively.

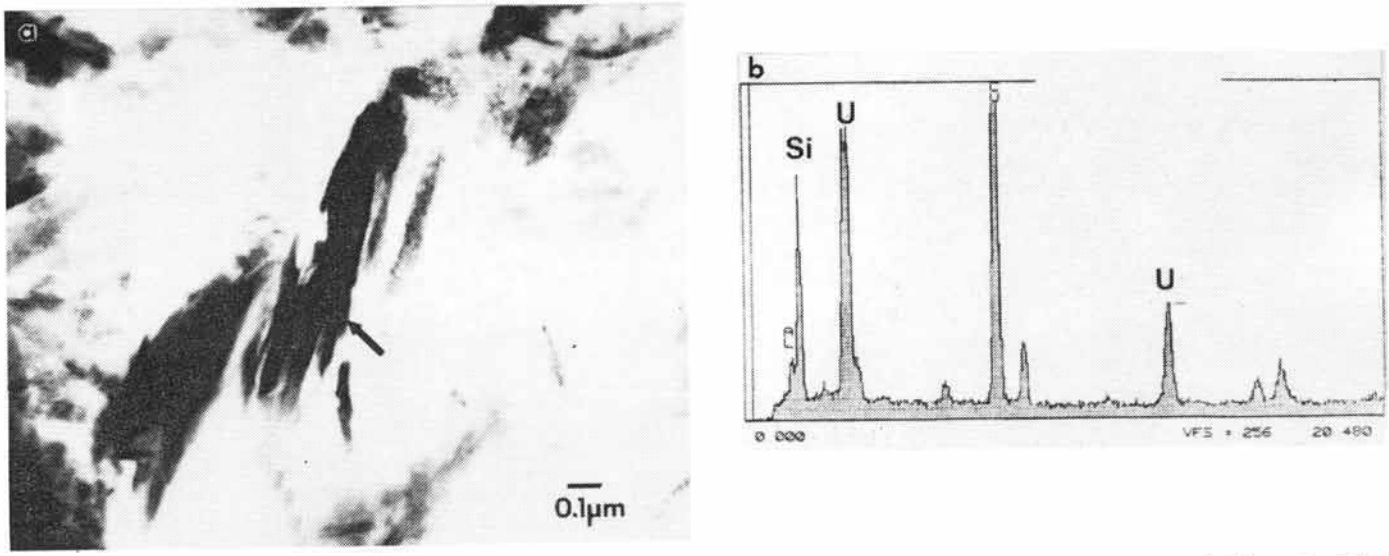

Fig. 3. Within the clay phases, uranium-rich silicate phases (arrow) were found (a) and identified as a uranyl silicate by SAED and (b) EDS compositional analysis.

observed. The uranium phosphate phase appeared to be connected to the uranium oxide, suggesting, that the uranium phosphate was an alteration product. The phase was identified, based on SAED data, as a tetragonal meta-autunite, uranyl phosphate hydrate $[M^{2+}(UO_2)_2(PO_4)_2 \bullet xH_2O]$, an alteration product of uraninite (2). Figure 6c displays an SAED pattern taken down the <001> zone axis of the uranium phosphate phase. The SAED identification of the

uranium-bearing phase has also indicated that the uranium is in the uranyl state [U(VI)].

The application of optical microscopy, SEM, and AEM techniques provided a clearer picture of uranium contamination at Fernald. The evidence suggests that some of the weathering processes at Fernald have resulted in the alteration of the initial uranium-bearing phases, and that soluble uranium interacted only slightly with the clay phases in the soil substrate, based on the detection limit for the EDS system. Effective removal of uranium from the Fernald soils will depend on detailed knowledge of the chemical and physical characteristics of the waste and its environment. The characterization methods described above, in combination with other methods under development (1), will allow remediation technology groups to find a more direct and efficient route to removing the contamination. These techniques are intended to be transferred for implementation throughout the contaminated sites of the DOE and private sector. For example, at Johnston Atoll (13) and Hanford (14) are areas were similar techniques may be applied.

CONCLUSION

Selected soil samples from SP4 and SP10 were examined using optical microscopy combined with SEM and AEM. With these methods we were able to isolate and characterize discrete uranium-bearing phases in the Fernald soils. With optical microscopy, no large uranium-bearing secondary minerals were observed. With SEM, however, clumps of uranium-rich regions were identified. Upon further examination with AEM, these regions were found to be composites of finely dispersed phases, which were both crystalline and amorphous. Little uranium was associated with the clay substrate itself. The types of uranium-bearing phases observed at Fernald are similar in many cases to those found in other environments, such as the amorphous uranium iron oxides phases and the altered uraninite. While it is still necessary to show the applicability of these results to larger soil samples, the utility of using multiple techniques for uranium phase identification and characterization has been demonstrated.

Further studies are underway of core and processed samples from Fernald to investigate the effectiveness of separation processes by characterizing the uranium bearing phases isolated.

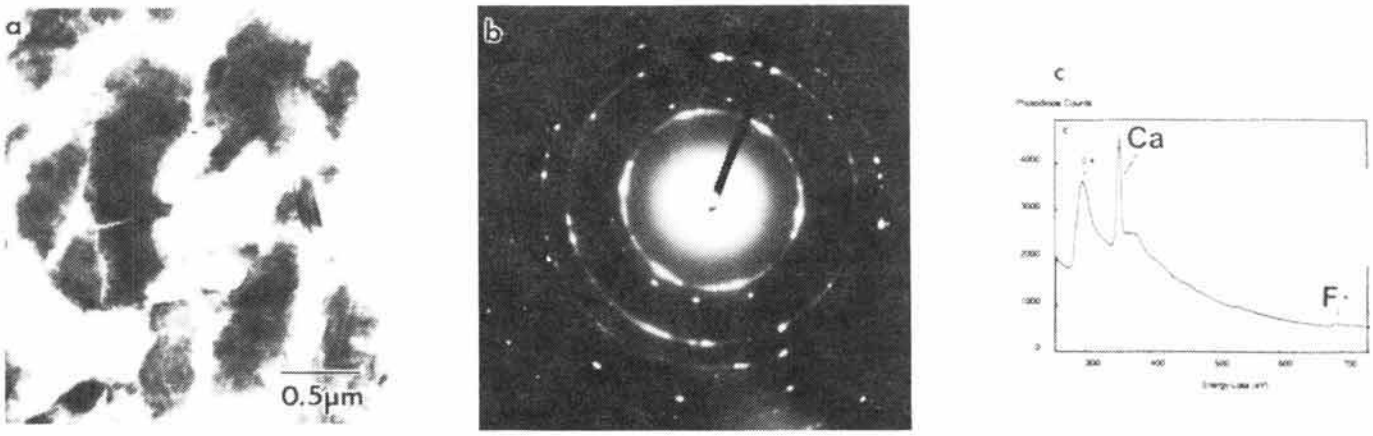

Fig. 4. Bright-field micrograph of uranium-bearing phases, (a) which were identified as fluorite by (b) SAED and (c) EELS analysis which shows the Ca-$L_{2,3}$ edges and F-K edge.

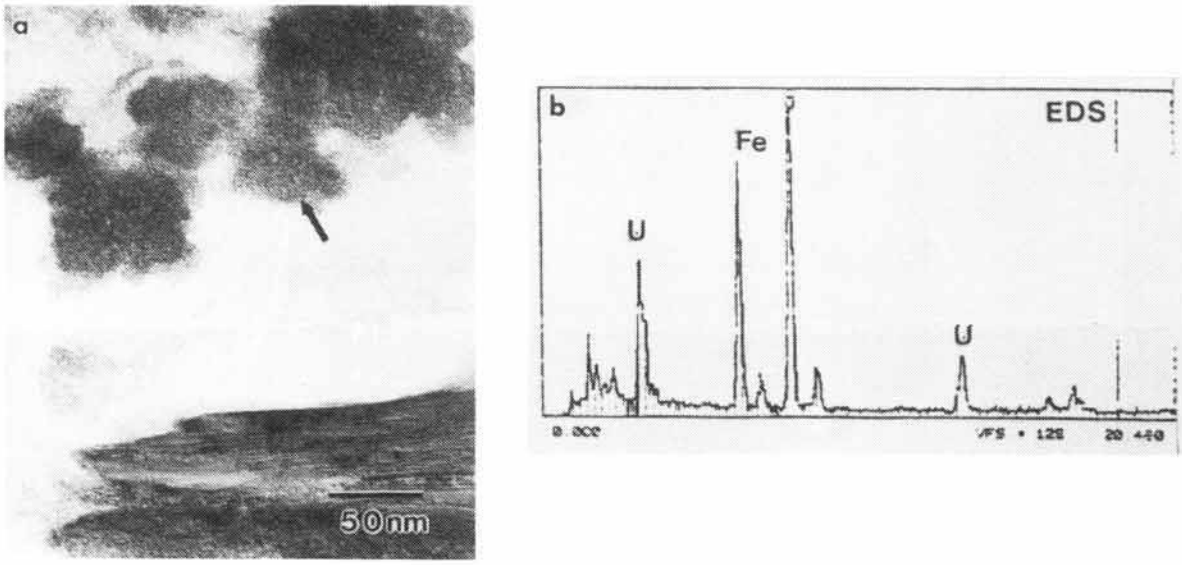

Fig. 5. (a) Amorphous iron oxide phase (arrow) found in SP4 in close proximity to clay. The EDS compositional analysis is shown in (b).

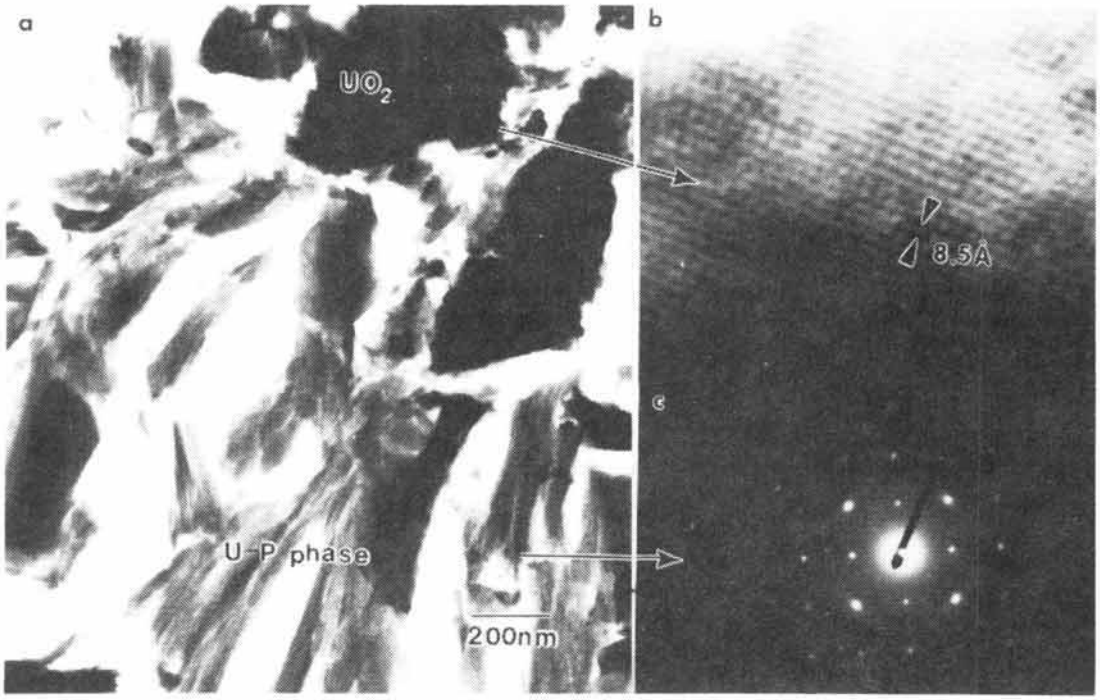

Fig. 6. Density separated uranium contaminated soils (SP10) contained two major phases (a), a uranium oxide and uranium phosphate. The darker clumps were identified as uranium oxide (UO_{2+x}). (b) A lattice image taken down a major pole shows spacings from the nonstoichiometric oxide, and attached to these were uranium phosphate crystallites. AEM determined the phosphate phase to be a tetragonal autunite, uranyl phosphate hydrate, by (c) SAED taken down the <001> zone axis.

ACKNOWLEDGMENTS

Work supported by the U.S. Department of Energy, Office of Technology Development, as part of the Uranium in Soils Integrated Demonstration Program, under contract W-31-109-ENG-38. Isolation of uranium by density differences was done by D. Chaiko (Argonne National Laboratory).

REFERENCES

1. J. C. CUNNANE, S. Y. LEE, D. L. PERRY, V. C. TIDWELL, V. GILL, and M. MICKELSON, "Field Demonstration of Technologies for Characterization of Uranium Contamination in Surface and Subsurface Soils," in these proceedings, Waste Management '93, Tucson, AZ.
2. L. H. JOHNSON and D. W. SHOESMITH, "Spent Fuel," in Radioactive Wasteforms for the Future, LUTZE, W, EWING, R. C., Eds.; Elsevier, p.665 (1988).
3. S. Y. LEE and J. D. MARSH, "Characterization of Uranium Contaminated Soils from DOE Fernald Environmental Management Project Site: Results of Phase I Characterization," ORNL/TM-11980, Oak Ridge National Laboratory (1992).
4. M. A. HAYAT, "Principles and Techniques of Electron Microscopy: Biological Applications," 3rd ed., CRC Press Inc., Boca Raton, FL (1989).
5. D. KAY, "Techniques for Electron Microscopy," Blackwell Press, Oxford, (1965).
6. K. WADA and W. KAKUTO, "Chloritized vermiculite in Korean Ultisol Studies by Ultramicrotomy and Transmission Electron Microscopy," Clays and Clay Minerals 37, 263 (1989).
7. D. FROSCH, C. WESTPHAL,and K. BACHHUBER, "A Determination of Thickness and Surface Relief in Reembedded Sections of an Epoxy and a Melamine-Resin containing Ferritin as Size Standard," Ultramicroscopy 17, 141 (1985).
8. D. PERRET, G. G. LEPPARD, M. MULLER, N. BELIZE, R. de VITRE, J. BUFFLE, "Electron Microscopy of Aquatic Colloids: Non-Perturbing Preparation of Specimens in the Field," Water Research 25, 1333 (1991).
9. L. L. AMES, J. E. McGARRAH, and B. A. WALKER, "Sorption of Uranium and Radium by Biotite, Muscovite, and Phlogopite," Clays and Clay Minerals 31, 343 (1983).
10. D. J. WRONKIEWICZ, J. K. BATES, T. J. GERDING, E. VELECKIS,and B. S. TANI, "Uranium Release and Secondary Phase Formation during Unsaturated Testing of UO_2 at 90°C," J. Nucl. Mater. 192, 107 (1992).
11. R. J. FINCH and R. C. EWING, "The Corrosion of Uraninite under Oxidizing conditions," J. Nucl. Mater. 190, 133 (1992).
12. C-K. HSI and D. LANGMUIR, "Adsorption of Uranyl onto Ferric Oxyhydroxides: Application of the Surface Complexation Site-Binding Model," Geochim. Cosmochim. Acta 49, 1931 (1985).
13. E. T. BRAMLITT, "Plutonium Mining for Cleanup," Health Physics 55, 451 (1988).
14. J. C. SHEPPARD, M. J. CAMPBELL, J. A. KITTRICK, and T. L. HARDT, "Retention of Neptunium, Americium, and Curium by Diffusible Soil Particles," Environ. Sci. and Technol. 13, 680 (1979).

means of addressing this problem is the development of real-time field screening technologies capable of providing data at high spatial resolution. Use of such techniques would minimize the total number of soil samples that must be collected, as well as reduce the number of sampling phases. Along these lines, four field-screening technologies for delineating the distribution of uranium contamination in surface and shallow subsurface soils have been tested and evaluated relative to their suitability for use in CERCLA and RCRA investigations (1). These technologies are high-resolution gamma-ray spectroscopy, wide-area beta scintillation counting, laser ablation-inductively coupled plasma-atomic emission spectroscopy (LA-ICP-AES), and long-range alpha detection (LRAD). Each of these technologies was tested under field conditions at selected locations at the FEMP during the late summer and early fall of 1992. This paper describes the field testing program, presents an initial evaluation of the results obtained, and discusses the conclusions drawn concerning the performance of each of the four technologies.

DESCRIPTION OF SCREENING TECHNOLOGIES AND FIELD DEMONSTRATION PROGRAM

Each of the four screening technologies was used to measure the uranium concentration (expressed in pCi/g) on a sampling grid with 18 m centers. Two sites were selected at the FEMP, the drum bailing area and the incinerator area. Uranium contamination at the drum bailing area stems from the past washing of contaminated drums and other articles, as well as air-borne deposition from milling and machining activities conducted in a nearby production area. Contamination at the incinerator area is primarily the result of emissions from the incineration of uranium-contaminated combustibles. Soil samples were also collected from each area, and analyzed in the laboratory to determine the uranium concentration. Because of the intended usage of these sampling data as benchmark comparisons for the field measurements, they will be referred to as "validation data" for ease of reference. The sampling grid for the soil samples were established according to standard FEMP protocols and does not correlate directly with the grid for the field screening demonstration. The goal of the demonstration was not to make a point-by-point comparison, which would be of little use given the vast differences in the scales of measurement. Rather, the desire was to compare the site-wide distribution of uranium contamination as determined by the four screening technologies with that for the soil sampling effort. Since the focus of this paper is on the field testing campaign, a brief summary of each of the field measurement techniques follows.

Field demonstration of the high-resolution gamma-ray spectroscopy system was conducted by personnel from the Pacific Northwest Laboratories (PNL). The system is based on the use of a germanium diode that may be collimated by specially shaped heavy metal shields. For the field demonstration, spectrometers were configured for both surface and downhole measurements. In the surface monitoring mode, the detector was suspended one meter above the ground by a tripod, and a large concave shield was placed over the detector to collect data from an area of approximately 100 m^2. In this configuration, the spectrometer detects uranium in the exposed surface and subsurface soils to a depth of approximately 40-50 cm, but the sensitivity decreases with depth due to gamma-ray attenuation.

The wide-area beta scintillation counter was developed at PNL to measure uranium concentrations in surface soils on a real-time basis. The system consists of multiple layers of plastic scintillating material for the measurement of beta particles from surficial soils (~the top 1 cm). The plastic scintillating layers are designed to measure uranium-238 surface concentrations by detecting the 2.29 MeV (maximum energy) beta particles from 234m-protactinium, a daughter product of uranium-238 decay. The system is designed to discriminate between high-energy beta particles and other interfering background radiation by using coincidence counting techniques, which identify high-energy beta particles by the depth to which they penetrate into the phosphor layer stack. The device used in the field tests was designed to monitor a surface area of approximately 0.1 to 0.2 m^2.

The LA-ICP-AES technique is a proven laboratory analytical method that has been adapted by Ames Laboratory for field applications (2). A neodymium YAG laser is used to ablate a small sample of in situ soil (~10-20 μg), while an argon gas stream entrains the ablated sample particles and transports them directly into the ICP. The atomic emission from the ICP is transferred by fiber optics to a spectrometer for quantitative analysis of total uranium. During the course of an individual measurement, the ablating laser beam is rastered over a sampling area of about 6.5 cm^2.

LRAD system, which was developed at Los Alamos National Laboratory, detects alpha particles (and other ionizing radiation) by collecting and measuring the ions that are produced when alpha particles are stopped in air. (3) Because the ambient air is the "detector gas," the field LRAD system was configured to be set directly on the ground. In this configuration, it detects the uranium in the surface soil by monitoring the air ionization near the soil surface. The LRAD system tested at FEMP was designed to monitor contamination present on an ~1m^2 of surface.

From August to September 1992, the four field-screening technologies described above were tested under field conditions at FEMP. The wide-angle gamma-ray spectrometer was demonstrated in the surface detection mode only at the drum bailing area. Measurements were not made at the incinerator area due to equipment difficulties. In contrast to gamma-ray spectrometry, the LA-ICP-AES tests were conducted only at the incinerator area. The LRAD and beta counter were used to measure surface concentrations at both areas. However, due to muddy and irregular ground surface conditions, measurements were not obtained from all pre-selected sampling locations.

RESULTS AND DISCUSSION

Available data from the field demonstration studies are compiled in Figs. 1a and 1b for the drum bailing and the incinerator areas, respectively. These figures also compile the soil sampling validation data. *Concentration* isopleth maps, based on the results obtained from the validation samples, are shown in Figs. 2a and 2b for the drum bailing and incinerator areas, respectively. These data are compiled here as a basis for discussion of the performance of each technology in measuring uranium concentrations under actual field conditions. More detailed discussions of the results obtained with the individual technologies will be published elsewhere.

The assessment of each technology is based on intercomparison of the analytical results obtained by the individual techniques and comparison of the field measurement results

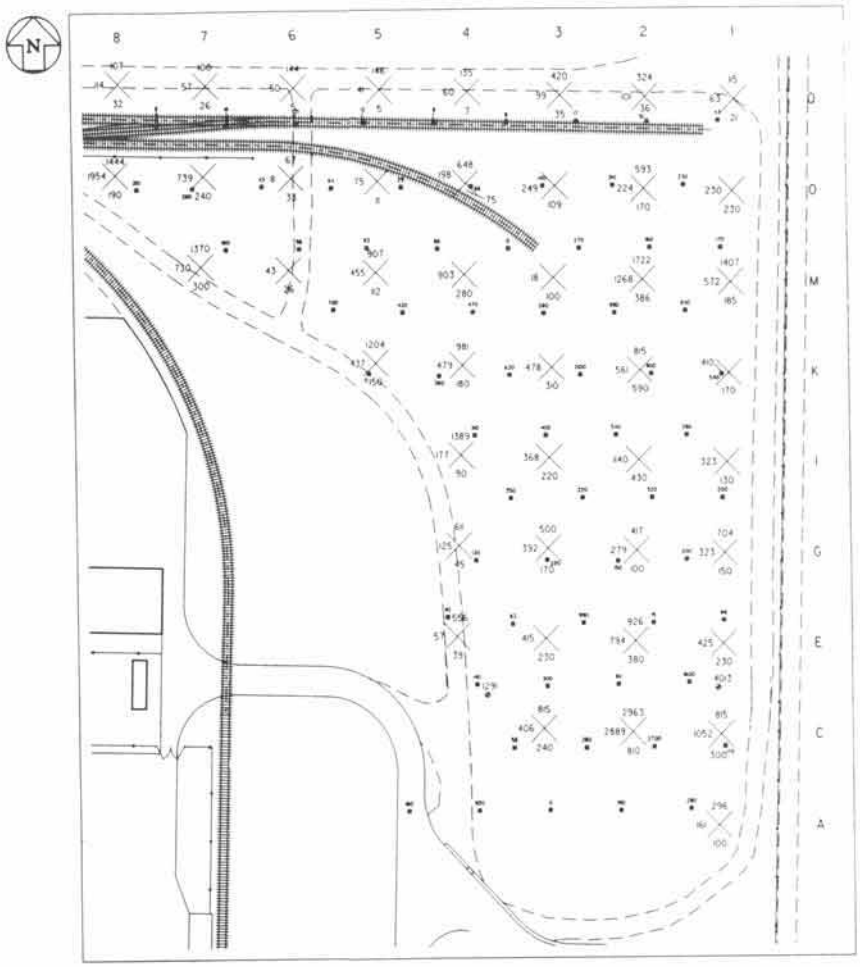

Figs. 1a and 1b. Compilation of field measurement data and validation data for the drum bailing (1a) and incinerator (1b) areas.

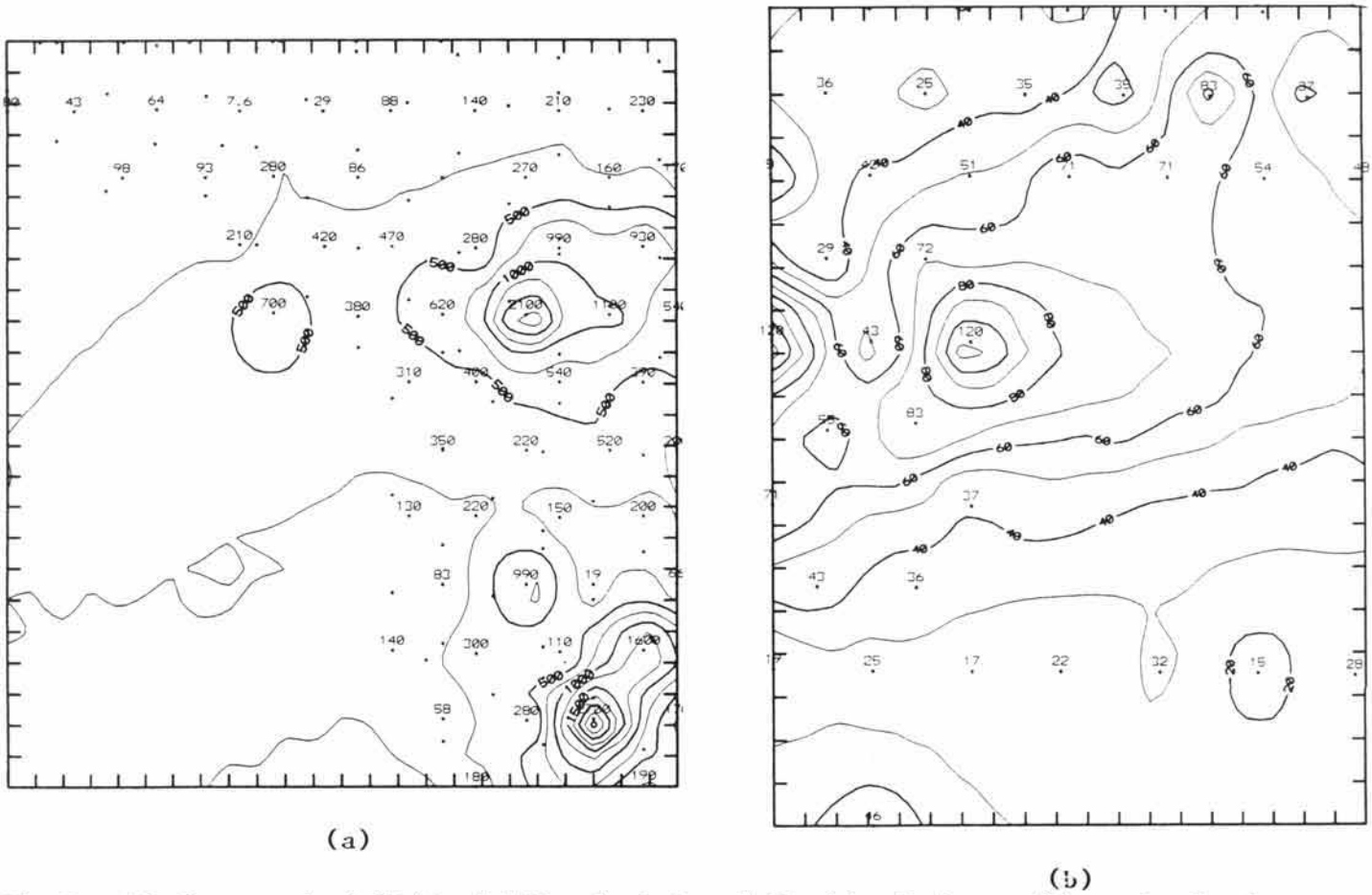

(a) (b)

Figs. 2a and 2b. Concentration (pCi/g) Isopleth Maps for the Drum bailing (a) and incinerator (b) areas based on the validation data.

with the laboratory validation data (Figs. 1a and 1b). Although factors such as cost and reliability will be very important in final evaluations of the suitability of any of these techniques for specific applications, the focus here is on how well each technique is able to measure the uranium contamination distribution. To facilitate comparisons, the measured uranium concentrations were expressed in units of pCi/g. The calibrations required to convert the detector responses into such concentration units introduced errors, which are discussed later.

We begin our analysis of the results by comparing the data in terms of the decision that they will be used to defend, that is, which soils exceed regulatory standards for uranium contamination. Although much uncertainty exists concerning the actual standard, probable limits will likely fall somewhere in the range of 100 pCi/g to background. Regardless of the actual standard, the results of this study are the same. In reviewing the field and validation data for the drum bailing area, each of the characterization methods consistently predicts that the soils will exceed the assumed range for the regulatory standards, except along the far north boundary of the site (Fig. 1a). However, in the incinerator area, where uranium concentrations are much lower (Fig. 1b), significantly different decisions would be made concerning the soils requiring remediation, depending on which field screening technology data set is used (unless the standard were set at or near background). This is a very important finding, because sites, such as the incinerator area, where contamination is widely distributed at levels near the *regulatory standard*, would benefit the most from field screening techniques. Development of novel sensor systems must be done in conjunction with gaining an understanding of how the acquired information relates to other field screening data, laboratory data, and the regulatory standard. In the paragraphs that follow, we outline in a preliminary fashion some of the steps that can be taken in interpreting the various similarities and differences noted in the five data sets.

One-to-one comparisons between the results obtained by the various techniques are illustrated by the scatter plots shown in Figs. 3 and 4. Figure 3 shows comparisons of results between gamma spectroscopy and beta scintillation counting (Fig. 3a), gamma spectroscopy and LRAD (Fig. 3b), and beta scintillation counting and LRAD (Fig. 3c) for the drum bailing area. Corresponding plots for the LA-ICP-AES technique are not provided because measurements were not made at the drum bailing area. Similar scatter plots for the incinerator area data obtained using beta scintillation counting, LRAD, and LA-ICP-AES are shown in Fig. 4. As mentioned earlier, gamma spectroscopy data were not obtained for the incinerator area because of some operational problems encountered during the field measurements. The data in Figs. 3 and 4 show significant scatter, particularly for the incinerator area, and the slopes of the regression lines differ significantly from one. Interpretations of these observations are discussed below.

Although the compared measurements for the four technologies were made at the same grid locations, the observed scatter in the data may be due to either local inhomogeneities in the actual uranium concentration or to measurement artifacts. Unfortunately, the available data are not sufficient

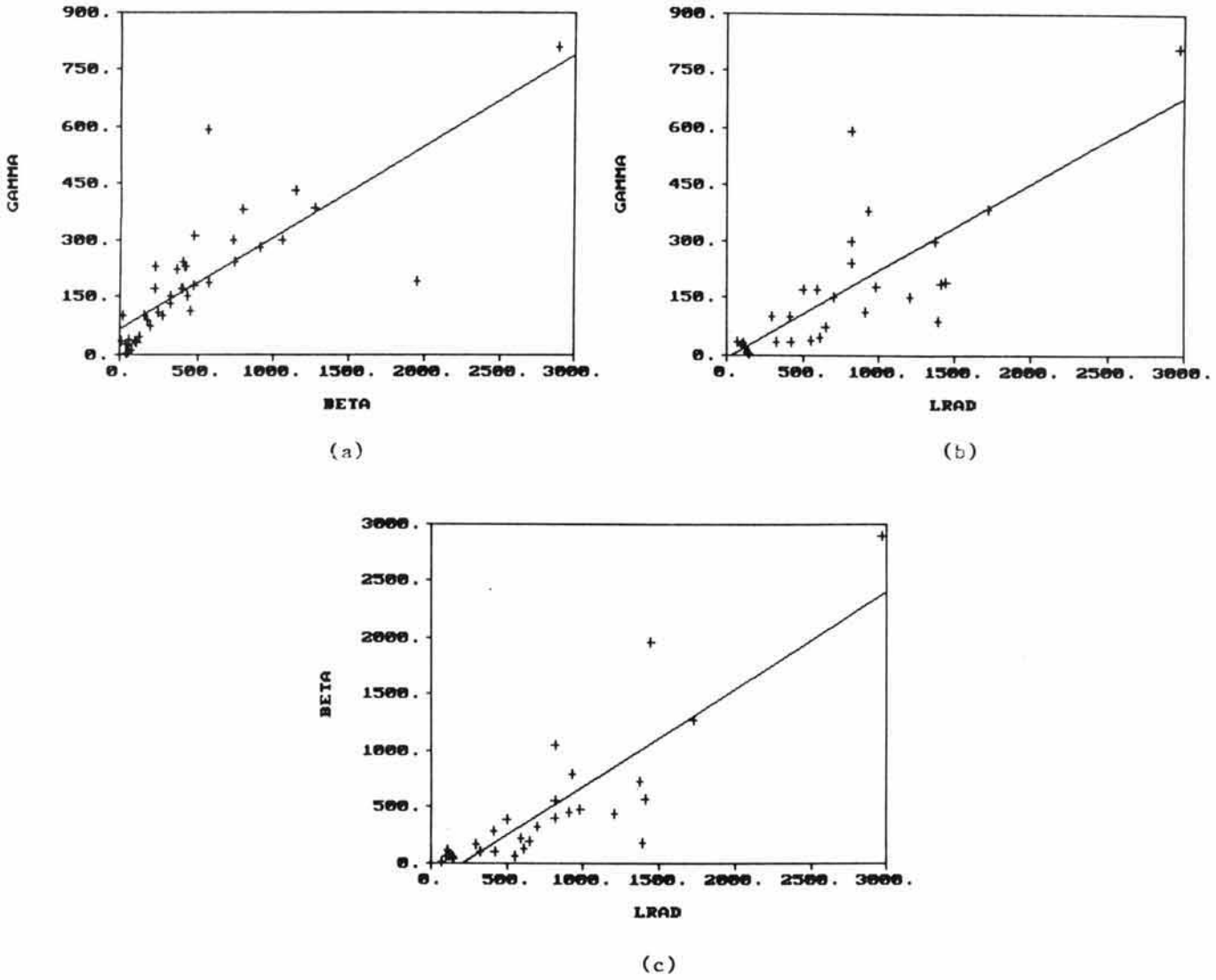

Figs. 3a, 3b, and 3c. Scatter plots for uranium concentration (pci/g) data obtained by three techniques from the drum bailing area.

to discriminate between these possibilities. The measured concentrations are not point concentrations but average concentrations for probed volumes that vary significantly for the individual measurement techniques. As pointed out above, the surface areas to which the techniques are sensitive vary from a few square centimeters to several tens of square meters. Also, the LA-ICP-AES and LRAD techniques are sensitive to uranium contamination on the surface of the exposed soil particles; the beta scintillator, perhaps to a depth of a few millimeters from the exposed surface; and the gamma spectroscopy technique, to a depth of several tens of centimeters. Because other FEMP characterization results (4,5) indicate that the contamination is heterogeneously distributed on the scales probed by the field measurement techniques much of the observed data scatter can probably be ascribed to these heterogeneities.

Although the data in Fig. 3 exhibit a general linear correlation, the linear regression lines have slopes significantly different from one. This is particularly true for the comparisons of the LRAD and beta scintillator measurements with the gamma spectroscopy measurements. The slope of the regression line for the beta scintillator/LRAD scatter plot is, however, much closer to the expected value of one (Fig. 3c). These results are consistent with the uranium contamination being concentrated close to the surface. Because the concentration results from gamma spectroscopy are calculated assuming a uniform uranium distribution as a function of depth, the calculated concentrations are lower than the actual surface concentrations. This results from averaging the uranium concentration over a much larger volume than the actual volume near the surface in which the uranium is concentrated.

Since a variety of unverified assumptions concerning the distribution of the uranium contamination are inherent in calibrating each of the systems tested, we decided to compare the techniques on a relative basis. One way to do this is to plot and compare the quartiles for the results obtained using each technique. To generate these plots, the population of measurements for each technique is divided into four intervals, each of which contains one-quarter of the total population. The quarter in which each measurement falls is identified in "quartile" plots to facilitate data comparisons. The quartile plots for both the drum bailing and the incinerator areas are shown in Figs. 5a and 5b, respectively. In general, these plots indicate that the techniques give fairly consistent results,

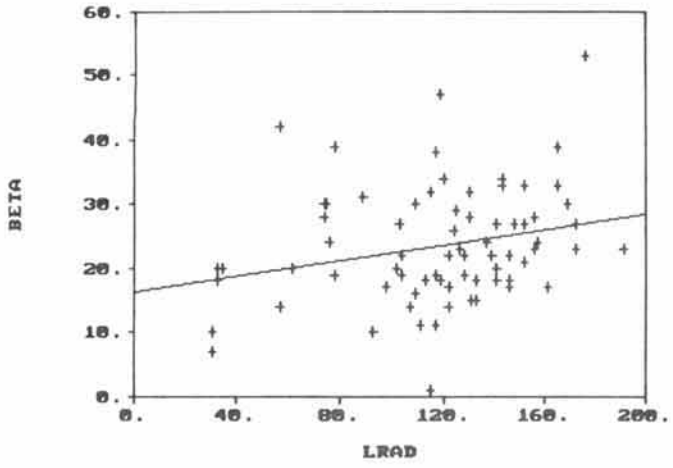

(a)

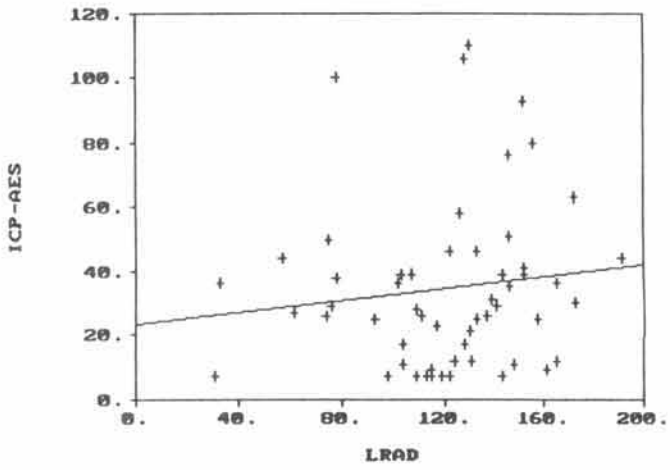

(b)

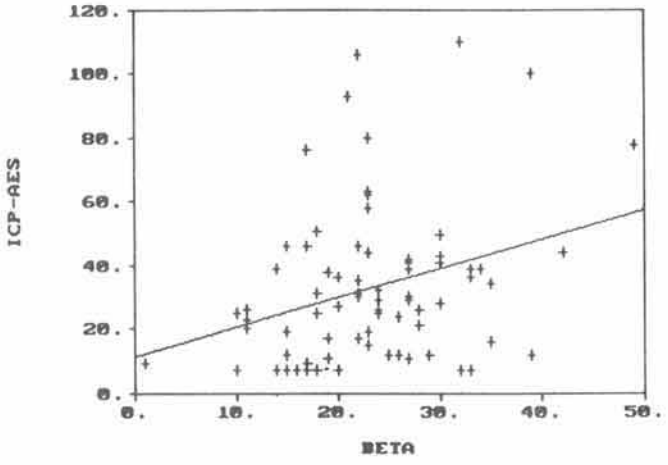

(c)

Figs. 4a, 4b, and 4c. Scatter plots for uranium concentration (pci/g) data obtained by three techniques from the incinerator area.

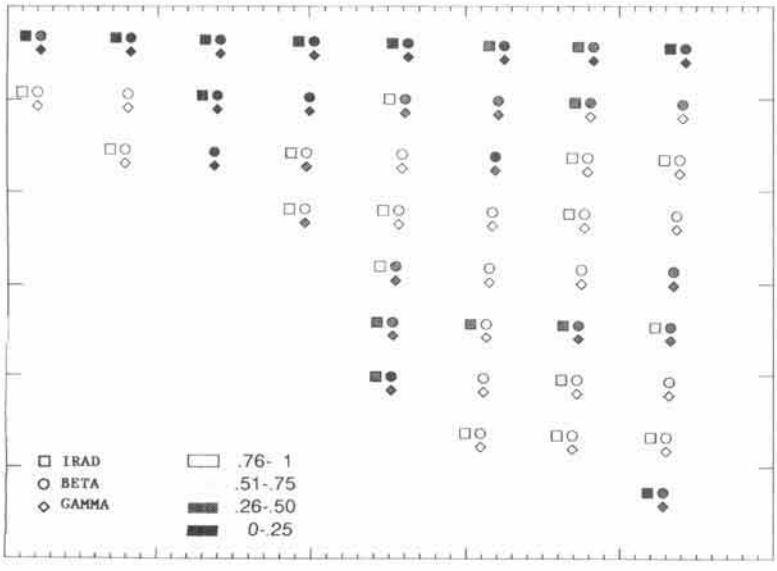

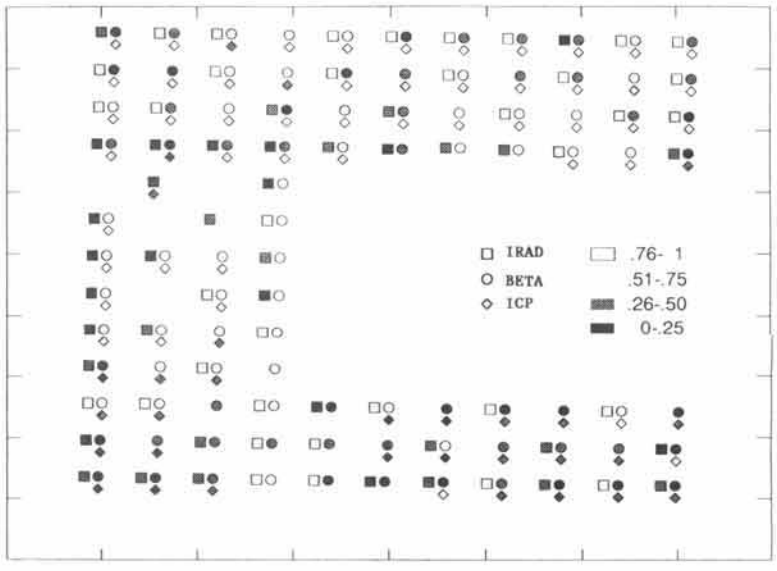

Fig. 5a and 5b. Quartile plots for the field data obtained from the drum bailing (a) and incinerator (b) areas.

indicate that the techniques give fairly consistent results, particularly for the drum bailing area, where the uranium concentrations are highest. Also, the results are, in general, consistent with the validation data in Fig. 2a and 2b. The reasons for the inconsistencies that are observed cannot be determined from the available data but are probably due, at least in part, to inhomogeneities in the actual uranium concentration distribution.

CONCLUSIONS

Although it is premature at this point to reach any final conclusions concerning the characteristics of the various technologies that were tested, several preliminary conclusions can be drawn from the initial field testing experience and the data analysis. The field testing did demonstrate that prototype systems for each of the technologies could be assembled in a configuration suitable for field deployment. Each of the systems was successful in quickly obtaining meaningful field screening data, despite the fact that a variety of operational problems were encountered, as might be expected with initial deployment of first-of-a-kind systems in the field. Unfortunately, possible local inhomogeneities in the uranium concentration distribution have made unambiguous interpretation of the observed differences between the field demonstration results impossible. However, the similarities in the relative concentration profiles, as determined for the different techniques, and the fact that most of the absolute concentration measurements are within an order of magnitude do suggest that all of the methods may be useful for specific field applications. Nevertheless, additional work is needed before definitive statements can be made concerning the practical usefulness of any of the techniques.

At this point, while the techniques may be useful for generating relative concentration contour maps, they will probably have to be used in conjunction with sampling data to establish the absolute values of the contours. Techniques with different position resolutions can be used in a complementary fashion in order to construct contouring data with different resolutions, as the specific needs involved demand. The observed scatter in the low concentration data for the incinerator area indicates that these techniques still require significant improvement if they are to be useful at the nominal target cleanup levels of 35 pCi/g.

ACKNOWLEDGEMENT

The work described in this report is supported by the Office of Technology Development of the Office of Environmental Restoration and Waste Management of the United States Department of Energy under the auspices of the Uranium in Soils Integrated Demonstration.

REFERENCES

1. FERNALD ENVIRONMENTAL MANAGEMENT PROJECT, "Uranium Soils Integrated Demonstration: Site Characterization Plan," PL-3022, Fernald, Ohio (September 1992).
2. A. P. D'SILVA, D. ZAMZOW, E. JASELSKIS, and S. WEEKS, "Remote, Real-Time Analysis of Hazardous Wastes Through Laser Ablation-Inductively Coupled Plasma-Atomic Emission Spectrometry," in Proceedings of SPECTRUM '92, Boise, ID, August 23-27, 1992, Vol. 1, pp. 409-413.
3. D. W. MacARTHUR and J. L. McATEE, "Long-Range Alpha Detector (LRAD)," in Proceedings of American Nuclear Society 1991 Winter Meeting, San Francisco, CA, November 10-14, 1991.
4. V. C. TIDWELL, S. Y. LEE, D. E. MORRIS, D. L. PERRY, C. CARNAHAN, J. C. CUNNANE, S. D. CONRADSON, V. GILL, and M. D. NICKELSON, "An Integrated Approach to the Characterization of Uranium-Contaminated Soils," presented at the SPECTRUM '92, Boise, ID, August 23-27, 1992, Vol. 1, pp. 221-227.
5. S. Y. LEE and J. D. MARSH, JR., "Characterization of Uranium Contaminated Soils from DOE Fernald Environmental Management Project Site: Results of Phase II Characterization," ORNL/TM-11980, Oak Ridge National Laboratory (1992).